Received November 12, 2020, accepted December 23, 2020, date of publication December 28, 2020,
date of current version January 7, 2021.

Digital Object Identifier 10.1109/ACCESS.2020.3047869

Architecture Modeling and Test of Tractor Power Shift Transmission

WU YIWEI[1], YAN XIANGHAI[1], AND ZHOU ZHILI[1,2]
[1]School of Vehicle and Traffic Engineering, Henan University of Science and Technology, Luoyang 471003, China
[2]Henan Key Laboratory of Vehicle Energy Saving and New Energy, Henan University of Science and Technology, Luoyang 471003, China

Corresponding author: Zhou Zhili (zzli@haust.edu.cn)

This work was supported in part by the National Key Research and Development Program of China under Grant 2016YFD0701002, in part by the Henan University of Science and Technology Innovation Talents Support Program under Grant 18HASTIT026, and in part by the Henan Province Production and Research Cooperation Project under Grant 182107000010.

ABSTRACT Architecture modeling, simulation, and test verification are performed to meet the requirements of multi-domain modeling and simulation of tractor power shift transmission (PST). The principles of architecture modeling and high level architecture (HLA) are analyzed, and the PST architecture modeling connotation and simulation system structure are studied. Then the dynamic principles of PST mechanical, hydraulic and control subsystems are analyzed in the preparation phase, sliding friction phase and holding phase of clutch engagement. To build the PST system simulation model, the simulation models and components of the three subsystems are established, and the object and interaction classes of the simulation object model (SOM) for each component are defined. After that, the parameter mapping relationship between the components is analyzed, the interfaces between the simulation components and HLA are encapsulated, and the simulation component running sequence is analyzed. Finally, the PST clutch engagement law under tractor shift conditions is simulated and tested. The relative error and correlation coefficient between the simulated and test data of shift solenoid valve drive current are used as indexes to evaluate the PST system simulation model. The results show that the simulated drive current curves are consistent with the test ones. The maximum error between the simulated and test shift time appears at the third gear downshift point, with a value of 7.89%, and the minimum correlation coefficient value between the simulated and the test drive current at all shift points is 0.92, which indicate that the PST system simulation model is effective and accurate.

INDEX TERMS Architecture modeling, high level architecture (HLA), power shift transmission (PST), test verification, tractor.

I. INTRODUCTION

The tractor power shift transmission (PST) is a mechanical, electrical, and hydraulic integrated system that integrates advanced technologies in many fields, such as machinery, hydraulics, and control. It is a complex product composed of multiple subsystems [1]. Using the architecture modeling method to establish a PST multi-domain system model and using the simulation platform to analyze and optimize its comprehensive performance can effectively reduce the model development and maintenance cycle and improve the efficiency of PST new product development [2]–[4].

Scholars have used different methods to carry out modeling and performance research on PST. In [5]–[8], the PST dynamic models were established with mathematical method and the PST shuttle and shift performance were studied. In [9], [10], the PST control and hydraulic simulation models were established respectively by using the MATLAB/Simulink and AMEsim software to study the PST control system performance. In [11], the PST simulation model was established by the Dymola software, and the control performance was analyzed using the MATLAB/Simulink software. The above researches only carried out performance analysis for a certain area of PST system, which could not fully reflect its multi-domain nature. Furthermore, the current research and application of architecture modeling method are mostly concentrated in the aerospace, aviation and military fields [12]–[14], while there are few researches in the field of agricultural tractors.

To meet the needs of tractor PST multi-domain modeling and simulation, we adopt the architecture modeling method to build the PST system simulation model by establishing the

The associate editor coordinating the review of this manuscript and approving it for publication was Lin Zhang.

PST mechanical, hydraulic and control subsystem simulation models and components, and use the method of combining simulation and test to evaluate the effectiveness and accuracy of the PST system simulation model.

II. ARCHITECTURE MODELING

A. MODELING PRINCIPLES

Architecture modeling takes the models established by different software in various fields as the main body, and the support environment as the model operation support carrier. By encapsulating the models into components that meet the architecture specifications, the interaction between models is realized by publishing/subscribing messages [15], [16].

High level architecture (HLA) is a general modeling and simulation integration framework recognized by the object management group (OMG) and IEEE, which can effectively support complex system modeling, and realize co-simulation analysis through run time infrastructure (RTI) [17]–[19].

B. PST ARCHITECTURE MODELING

PST architecture modeling refers to the systematic abstract analysis of PST based on the HLA object-oriented method, the establishment of mechanical, hydraulic and control simulation components, and the construction of the PST system simulation model by packaging the simulation components. Co-simulation is implemented in the HLA simulation system. Fig. 1 shows the HLA-based PST simulation system structure.

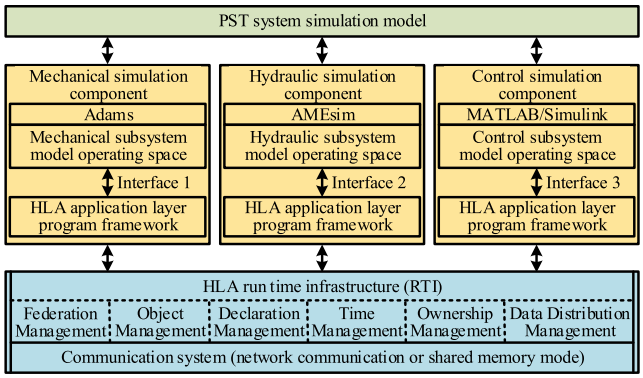

FIGURE 1. PST simulation system logic structure diagram.

In Fig. 1, the simulation components mainly involve the Adams, AMEsim and MATLAB/Simulink software. The interaction between models means that the model input/output is stored and taken out by the simulation components during the transmission process. Such operations are completed through the interface between the model and the HLA application layer program framework, with which the model is associated by defining interface operation functions. The HLA application layer program framework is the basis of the simulation component, whose main function is to initialize simulation component and model, and start software. RTI is the foundation for operation of the simulation system, which provides services such as federation management, object management, and declaration management [20].

III. PST SIMULATION COMPONENT CONSTRUCTION

The PST simulation component is established to integrate the input/output of the developed mechanical, hydraulic and control system model parameters, the operation of the model, and the simulation step advancement of the model into the operation process of the HLA simulation system in the form of calling functions. Through the call of model parameter input/output functions, interaction between models in different domains is realized. HLA uses object model templates to standardize the description of object models, including federation object model (FOM) and simulation object model (SOM), which can be used to describe system simulation model and simulation components respectively [21]. SOM defines the object class and interactive class information published/subscribed by the simulation component in the form of a table, and all SOMs are integrated as FOM [22].

A. PST MECHANICAL SIMULATION COMPONENT

The PST mechanical simulation component outputs dynamic parameters for the system simulation model, including the torque and speed of shafts, gears, clutches, synchronizers and bearings. Fig. 2 shows the power transmission of the PST mechanical subsystem.

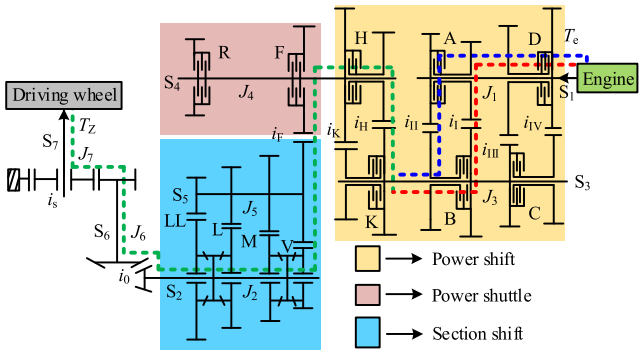

FIGURE 2. PST mechanical subsystem power transmission diagram.

In Fig. 2, the PST mechanical subsystem has 32 forward gears and 25 reverse gears, of which 4 shift clutches (A, B, C and D) and high and low gear (Hi and Lo) clutches (H and K) are combined into 8 power shifts, 2 shuttle clutches (F and R) form forward and reverse gears, and 2 synchronizers form four section shifts (LL, L, M and V). The section shift determines the shift section, and the power shift subdivides the transmission ratio within the section to realize the power shift within the section.

We take the forward Hi-V-I gear upshift to Hi-V-II gear as an example for dynamic analysis. It can be seen from Fig. 2 that when the PST is in Hi-V-I gear, clutches A, H and F are engaged, and power is transmitted through the red and green routes. When the PST is in Hi-V-I gear, clutches B, H and F are engaged, and power is transmitted through

the blue and green routes. When Hi-V-I gear is upshifting to Hi-V-II gear, clutch A is to be disengaged, clutch B is to be engaged, and other clutch states remain unchanged. According to different clutch states, the gear shift process is divided into preparation phase, sliding friction phase and holding phase. The three phases are analyzed below.

1) PREPARATION PHASE

The transmission torque of clutch A drops to the torque when it just does not slide, and the clearance of the friction plate of clutch B is just zero and no torque is transmitted. The dynamic equation of input shaft (S_1) is as follows:

$$T_e - T_A = J_1' \frac{d\omega_e}{dt} \tag{1}$$

In (1), T_e is the engine torque, N · m, T_A is the torque of clutch A, N · m, J_1' is the equivalent moment of inertia of S_1, kg · m^2, and ω_e is the engine angular velocity, rad/s.

Without considering system friction resistance, viscous resistance, and damping, the energy of all rotating parts in the PST is equal to the energy obtained from the engine, which can be calculated by (2).

$$E_e = \frac{1}{2}J_1'\omega_e^2 = \frac{1}{2}\omega_e^2\left[J_1 + \frac{J_3}{i_I^2} + \frac{J_4}{(i_I i_H)^2} + \frac{J_5}{(i_I i_H i_F)^2} + \frac{J_2}{(i_I i_H i_F i_V)^2} + \frac{J_6}{(i_I i_H i_F i_V i_0)^2} + \frac{J_7}{(i_I i_H i_F i_V i_0 i_s)^2}\right] \tag{2}$$

In (2), E_e is the total kinetic energy obtained from the engine, J, J_1, J_2, J_3, J_4, J_5, J_6, and J_7 is the moment of inertia of S_1, output shaft (S_2), driven shaft (S_3), shuttle shaft (S_4), intermediate shaft (S_5), bevel gear shaft (S_6) and final drive half shaft (S_7), respectively, kg · m^2, i_I, i_H, i_F, i_V, i_0, and i_s is the transmission ratio of each gear.

The torque of S_7 is described in (3).

$$T_Z = \frac{J_7}{i_I i_H i_F i_V i_0 i_s}\frac{d\omega_e}{dt} \tag{3}$$

2) SLIDING FRICTION PHASE

Clutch A starts to slide until the transmission torque drops to a sliding stop, and clutch B also starts to slide until the transmission torque exceeds the load. During this phase, both clutch A and clutch B are in a semi-engaged state, rotating relative to each other, and the friction plates generate heat. The dynamic equation of S1 is as follows:

$$T_e - T_A - \frac{T_B}{i_{II}} = J_1' \frac{d\omega_e}{dt} \tag{4}$$

In (4), T_B is the torque of clutch B, N · m.

The energy relationship between all rotating parts in the PST and the engine can be expressed by (5).

$$E_e = \frac{1}{2}J_1'\omega_e^2 = \frac{1}{2}J_1\omega_e^2 + \frac{1}{2}\omega_{A2}^2\left[\frac{J_3}{i_I^2} + \frac{J_4}{(i_I i_H)^2} + \frac{J_5}{(i_I i_H i_F)^2} + \frac{J_2}{(i_I i_H i_F i_V)^2} + \frac{J_6}{(i_I i_H i_F i_V i_0)^2} + \frac{J_7}{(i_I i_H i_F i_V i_0 i_s)^2}\right] + E_{AB} \tag{5}$$

In (5), ω_{A2} is the angular velocity of clutch A driven disc, rad/s, and E_{AB} is the energy consumed by clutch A and clutch B due to slide, which can be calculated by (6).

$$E_{AB} = \int_{t_0}^{t_1} T_A\left|\omega_e - \omega_{A2}\right| dt + \int_{t_0}^{t_1} T_B\left|\frac{\omega_e}{i_{II}} - \omega_{B2}\right| dt \tag{6}$$

In (6), t_0 and t_1 is the time when sliding friction starts and ends, respectively, and ω_{B2} is the angular velocity of clutch B driven disc, rad/s.

3) HOLDING PHASE

In this phase, the transmission torque of each clutch no longer changes. Clutch A has been disengaged and the transmission torque is zero, clutch B has been engaged, and the transmission torque has increased to the maximum torque that can be transmitted under system pressure. The dynamic equations are as follows:

$$T_e - \frac{T_B}{i_{II}} = J_1' \frac{d\omega_e}{dt} \tag{7}$$

$$E_e = \frac{1}{2}J_1'\omega_e^2 = \frac{1}{2}\omega_e^2\left[J_1 + \frac{J_3}{i_{II}^2} + \frac{J_4}{(i_{II} i_H)^2} + \frac{J_5}{(i_{II} i_H i_F)^2} + \frac{J_2}{(i_{II} i_H i_F i_V)^2} + \frac{J_6}{(i_{II} i_H i_F i_V i_0)^2} + \frac{J_7}{(i_{II} i_H i_F i_V i_0 i_s)^2}\right] \tag{8}$$

$$T_Z = \frac{J_7}{i_{II} i_H i_F i_V i_0 i_s}\frac{d\omega_e}{dt} \tag{9}$$

The dynamic model of PST mechanical subsystem shows the dynamic relationship between mechanical parts, which is the basis of PST dynamic performance simulation. The variables of dynamic model are the messages published/subscribed by PST mechanical simulation component.

The 3D model accuracy of PST mechanical subsystem has an important impact on the dynamic simulation results. We use Creo Parametric software to establish the 3D model and import it into Adams software as the HLA mechanical simulation component, named Mechanical. By subscribing to messages published by other simulation components, the mechanical subsystem dynamic simulation is performed. Mechanical interacts with other components through object classes and interaction classes. The SOM object class structure table defines the published/subscribed object class of components. Mechanical SOM object class includes subclasses such as shaft class, gear class, clutch class, synchronizer class, bearing class and load class. The SOM interaction class structure table defines the published/subscribed interaction class of components. Mechanical SOM interaction class includes subclasses such as start class, shift class, shuttle class and driving class. The start class includes subclasses of forward and reverse, the shift class includes subclasses of upshift, downshift and neutral, the shuttle class includes subclasses of forward to reverse and reverse to forward, and the driving class includes subclasses of forward driving and reverse driving.

B. PST HYDRAULIC SIMULATION COMPONENT

The PST hydraulic simulation component outputs hydraulic parameters for the system simulation model, including the hydraulic oil flow of the shift solenoid valve, piston displacement and speed, clutch friction plate pressure, pulse width modulation (PWM) cycle and duty cycle. Fig. 3 shows the pressure transmission of the PST hydraulic subsystem.

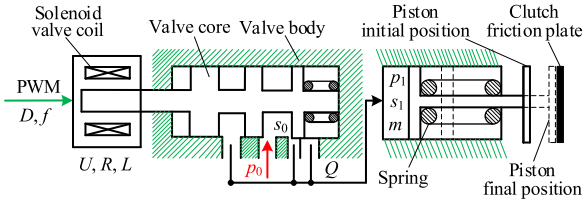

FIGURE 3. PST hydraulic subsystem pressure transmission diagram.

The PST hydraulic subsystem consists of a gear pump, a shift solenoid valve and an actuator. The transmission control unit (TCU) sends out a PWM signal to control the drive current of the shift solenoid valve and change the hydraulic oil flow, thus the speed and thrust of the actuator pushing the clutch change accordingly, and the disengagement and engagement speed and transmission torque of the clutch are accurately controlled. The relationship can be expressed by (10).

$$I = \frac{U}{2R}\frac{(1-A)(1-B)}{1-AB} \tag{10}$$

In (10), I is the drive current of the shift solenoid valve, A, U is the coil voltage of the shift solenoid valve, V, and R is the coil resistance of the shift solenoid valve, Ω. A and B can be calculated using (11) and (12).

$$A = \mathrm{e}^{-DR/fL} \tag{11}$$

$$B = \mathrm{e}^{-(1-D)R/fL} \tag{12}$$

In (11) and (12), D is the PWM signal duty cycle, f is the PWM signal frequency, Hz, and L is the coil inductance of the shift solenoid valve, H.

According to the current and flow characteristic curve of the shift solenoid valve, the hydraulic oil flow of the piston controlled by the shift solenoid valve under the system pressure can be obtained. The relationship between flow and pressure is as follows:

$$Q = \alpha s_0 \sqrt{2\,(p_1 - p_0)/\rho} \tag{13}$$

In (13), Q is the hydraulic oil flow, L/min, α is the valve port flow coefficient, s_0 is the flow area of the valve port in Fig. 4, m^2, p_1 is the piston chamber pressure, Pa, p_0 is the system pressure, Pa, and ρ is the oil density, $\mathrm{kg/m}^3$.

1) PREPARATION PHASE

The drive current that controls clutch A and the pressure in piston chamber decrease, and the transmission torque of clutch A decreases to the torque when it does not slide. During this phase, the piston displacement is zero. According to the piston force balance, the force of piston on clutch A is obtained as:

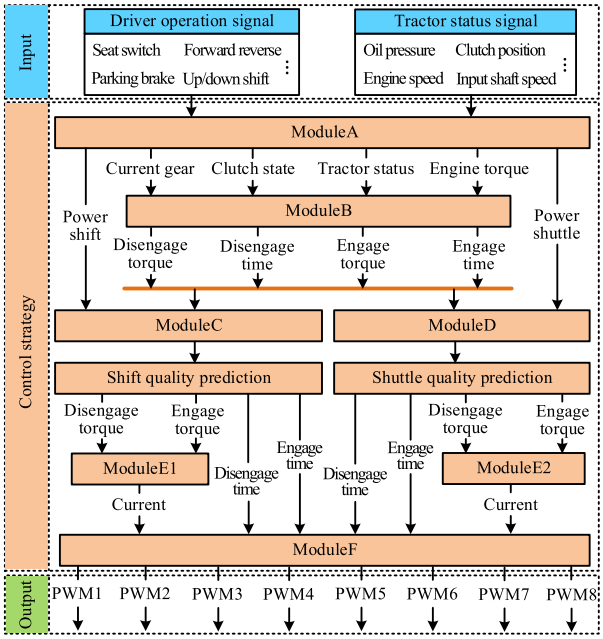

FIGURE 4. PST control subsystem principle diagram.

$$F_{\mathrm{A}} = p_1 s_1 - k\,(x_0 + x) \tag{14}$$

In (14), F_{A} is the force of clutch A, N, s_1 is the piston area, m^2, k is the piston spring stiffness, N/m, x_0 is the spring precompression, m, and x is the piston displacement, m.

The torque of clutch A can be calculated by (15).

$$T_{\mathrm{A}} = \mu r F_{\mathrm{A}} N \eta \tag{15}$$

In (15), μ is the friction coefficient, r is the friction action radius, m, N is the number of friction plate pairs, and η is loss coefficient of force from piston to clutch A.

The drive current that controls clutch B rises, and the pressure in piston chamber rises. The piston pushes the friction plate of clutch B to make the gap exactly zero, and no torque is transmitted. Taking the piston as the analysis object, we can establish the dynamic equation as follows:

$$mx + Cx + k\,(x_0 + x) = p_1 s_1 \tag{16}$$

In (16), m is the mass of piston, kg, C is the piston viscous damping coefficient.

2) SLIDING FRICTION PHASE

The drive current that controls the clutch A and the pressure in piston chamber continue to decrease until the transmission torque drops to a sliding stop. During this phase, the piston displacement is zero, and the force and transmission torque of clutch A still satisfy the relational equations (14) and (15). The drive current that controls the clutch B and the pressure in piston chamber continue to rise until the transmission torque exceeds the load. In this phase, the piston displacement is

zero. According to the piston force balance, the force of the piston on clutch B is obtained as:

$$F_B = p_1 s_1 - k\,(x_0 + x) \tag{17}$$

3) HOLDING PHASE

In this phase, clutch A has been separated, and the separation process satisfies (16). Clutch B has been engaged, the transmission torque has increased to the maximum torque that can be transmitted under the system pressure, and the force of clutch B still satisfies (17).

The PST hydraulic subsystem is composed of two subsystems: lubrication and control. The lubrication subsystem adopts pressure oil lubrication, and the lubricating oil flow of each part varies with the working status. The control subsystem uses high-pressure oil as the transmission medium, and controls the clutch engagement/disengagement through the proportional solenoid valve and the hydraulic cylinder actuator. We use AMESim software to establish the PST hydraulic subsystem model, name it Hydraulic as an HLA hydraulic simulation component, and perform hydraulic subsystem simulation by subscribing to the news published by other simulation components. The Hydraulic SOM object class include subclasses such as gear class, clutch class, synchronizer class, load class, PWM class and actuator class. The Hydraulic interaction class is consistent with the Mechanical one.

C. PST CONTROL SIMULATION COMPONENT

The PST control simulation component outputs control parameters for the system simulation model, including driver operation signal, tractor status signal and PWM signal. In the three phases of shift process, the PST control subsystem generates PWM signal, which is transmitted to the hydraulic and mechanical subsystems, and executes the corresponding actions to complete the shift. Fig. 4 shows the control principle of the PST control subsystem.

In Fig. 4, the input signal of the PST control subsystem includes the driver's operation signal and the tractor status signal. The control strategy is implemented by modules A, B, C, D, E (E1 and E2) and F. Module A determines the current gear, clutch status and driving direction according to input signal. Module B calculates the engagement/disengagement torque and time of the clutch according to the output parameters of module A and the engine torque. Module C and module D respectively predict the shift and shuttle quality according to the output parameters of Module B and the shift and shuttle signals output by Module A. By adjusting the clutch engagement/disengagement torque and time, the shift and shuttle quality is improved. Module E1 and module E2 convert clutch engagement/disengagement torque into drive current of the shift solenoid valve according to the adjustment result. Module F matches the clutch torque and time, and outputs 8 PWM control signals.

We use MATLAB/Simulink software to establish the PST control subsystem model, name it Control as an HLA control simulation component, and perform control subsystem simulation by subscribing to the news published by other simulation components.

The PST system simulation model is built by the established mechanical, hydraulic and control simulation components, as shown in Fig. 5.

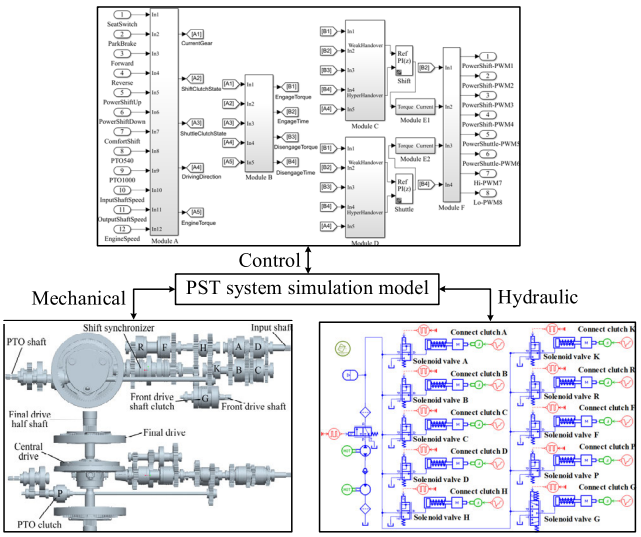

FIGURE 5. PST system simulation model.

D. PARAMETER MAPPING BETWEEN SIMULATION COMPONENTS

Object attributes and interaction parameters with consistent naming between simulation components belong to direct mapping. Mechanical load class object attributes are directly mapped with load component object attributes, and clutch class object attributes are directly mapped with Hydraulic clutch class object attributes.

The mapping relationship between shaft object attributes and pulse object attributes of Control is as follows:

$$n = 60a/M \tag{18}$$

In (18), n is the shaft speed, r/min, a is the number of pulses per second, and M is the measurement gear teeth.

The mapping relationship between torque attribute of Mechanical clutch and pressure attribute of Hydraulic clutch is described in (19).

$$T = \mu rpsN\eta \tag{19}$$

In (19), T is the clutch torque, N · m, p is the clutch pressure, Pa, and s is the clutch friction surface area, m^2.

The mapping relationship between the solenoid valve drive current attributes of the Hydraulic solenoid valve class and the duty cycle and period attributes of Control PWM class can be expressed by (10) to (12).

To ensure the correct mapping relationship between the clutch pressure and the drive current of the shift solenoid valve in Hydraulic, a calibration test is used to measure

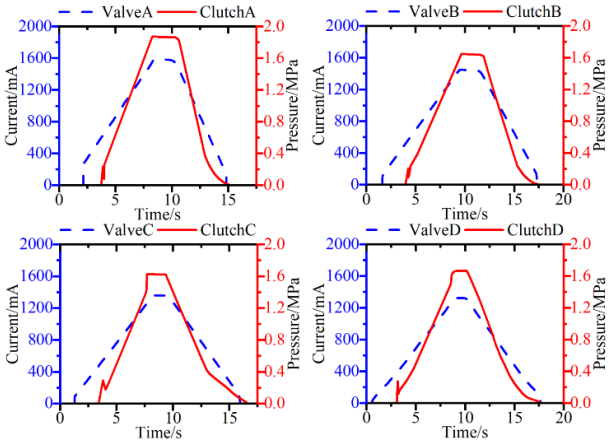

FIGURE 6. Mapping relationship between clutch pressure and solenoid valve drive current.

the relationship between the four clutch pressures and the corresponding drive current. Fig. 6 shows the test results.

E. SIMULATION COMPONENT HLA ENCAPSULATION

HLA encapsulation refers to the establishment of an interface between software and RTI. Adams, AMESim and MATLAB/Simulink have differences in data solution and data structure, so the methods of integrating them into the HLA system are different. By shielding the differences in the internal data of different software, we encapsulate the software and HLA interface, and realize the HLA general encapsulation of different simulation components. Here we utilize Adams custom subroutine interface, AMESim secondary development platform AMESet and MATLAB/Simulink S function. Table 1 shows the standardized functions and functions that implement the encapsulation.

TABLE 1. General encapsulation standardized functions.

Name	Function
Initialize module ()	Software startup and simulation component initialization
Time advance ()	Simulation component step drive
Get value ()	Get output variable value after step update from software workspace
Put value ()	Put value after data exchange into workspace
End module ()	Software shutdown and simulation component processing

F. SIMULATION COMPONENT RUNNING SEQUENCE

According to the HLA time management mechanism [23], the time management strategies of mechanical, hydraulic and control simulation components are set to both time control and time constraint. The types of sending events are timestamp order (TO), the simulation time advancement methods are based on the step size, the amount of time lookahead is zero, and the three components run on the same computer to provide synchronization time constraints. Fig. 7 shows the logic relationship of the simulation component running sequence.

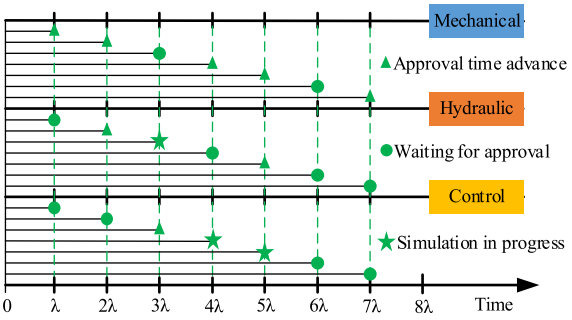

FIGURE 7. Simulation component running sequence relationship.

In Fig. 7, the simulation steps of Mechanical, Hydraulic and Control are λ, 2λ and 3λ respectively, and time λ is the synchronization point. At time λ, the three simulation components simultaneously apply to the RTI for the time advancement of their respective simulation steps. The maximum time advance safety value of the simulation component, that is, the lower bound on time stamp (LBTS) is as follows [24]:

$$LBTS_i = Min\left(W_j + Lookahead_j\right) \tag{20}$$

In (20), $LBTS_i$ is the lower bound on time stamp of the simulation component F_i, W_j is the current simulation time of the simulation component F_j that can send TO events to F_i, and $Lookahead_j$ is the time forward value of F_j.

From (20), it can be obtained that $LBTS_1$ of Mechanical is 3λ, $LBTS_2$ of Hydraulic is 2λ, and $LBTS_3$ of Control is 2λ at time λ. Mechanical application time is 2λ, which is less than 3λ, RTI approves its application. Hydraulic and Control application times are 3λ and 4λ, which are greater than 2λ, therefore, Hydraulic and Control applications enter the waiting state. At time 2λ, Mechanical completes the simulation step time advance and applies to RTI for the next time advance. At this moment, $LBTS_1$, $LBTS_2$, and $LBTS_3$ are all 3λ, RTI approves Mechanical and Hydraulic applications, and the Control application is still waiting. At time 3λ, Mechanical completes the simulation step time advance, and Hydraulic is in simulation operation. At this moment, $LBTS_1$ is 3λ, $LBTS_2$ is 4λ, and $LBTS_3$ is 4λ, RTI approves the Control application, and the Mechanical application is in a waiting state. At time 4λ, Hydraulic completes the simulation step time advance, and Control is in simulation operation. At this moment, $LBTS_1$ is 6λ, $LBTS_2$ is 5λ, and $LBTS_3$ is 5λ, RTI approves Mechanical application, and Hydraulic application is waiting. The three components loop the above process until the end of the simulation.

IV. PST SYSTEM SIMULATION MODEL VERIFICATION

PST clutch engagement law mainly refers to the change law of clutch torque, which is the basis for formulating PST start, shift and shuttle strategies, and is one of the important properties of PST [25]. Aiming at the tractor's upshift and downshift

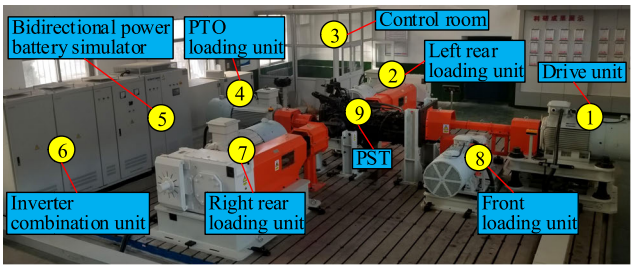

FIGURE 8. PST test bench.

conditions during the clay plowing operation, we use HLA simulation system to simulate the clutch engagement law. The simulation gear is set to Lo, the section is L, the starting condition gear is Lo-L-I, and the engine is in the calibration mode. The PST input speed is 2200r/min, the input torque is 550N · m, and the PST hydraulic component pressure is 22bar. Then we compare and analyze the results with the PST bench test ones to verify the effectiveness of the PST system simulation model. Fig. 8 shows the PST test bench, which is used to test the clutch engagement law. The relative error and correlation coefficient between simulation and test results are used as indexes to evaluate the accuracy of the PST system simulation model.

A. EVALUATION INDEX

The relative error between simulation and test results is defined as:

$$\varepsilon = \frac{|T - S|}{T} \times 100\% \tag{21}$$

In (21), ε is the relative error, T is the test value, and S is the simulation value.

We performed statistical analysis on the time series of simulation and test data to obtain the maximum, minimum, mean, standard deviation and root mean square values of the two sets of data, forming two sets of series X_i and Y_i, the expressions are as follows:

$$X_i = [x_1, x_2, x_3, x_4, x_5] \tag{22}$$

$$Y_i = [y_1, y_2, y_3, y_4, y_5] \tag{23}$$

The correlation coefficient between X_i and Y_i can be expressed by (24).

$$z_i = \frac{\min |x_i - y_i| + \xi \max |x_i - y_i|}{|x_i - y_i| + \xi \max |x_i - y_i|} \tag{24}$$

In (24), z_i is the correlation coefficient of each characteristic parameter and ξ is the resolution coefficient with a value of 0.5.

The correlation coefficient z between simulation and test data is the average of the correlation coefficients of all characteristic parameters, it can be calculated using (25).

$$z = \frac{1}{5} \sum_{i=1}^{5} z_i \tag{25}$$

TABLE 2. The relationship between the correlation degree and correlation coefficient.

Level	Correlation coefficient range	Correlation degree
1	$z \in [0, 0.3]$	Smaller
2	$z \in (0.3, 0.5]$	Small
3	$z \in (0.5, 0.7]$	Big
4	$z \in (0.7, 0.9]$	Bigger
5	$z \in (0.9, 1]$	The biggest

We divided the correlation degree between simulation and test data into 5 levels according to the range of correlation coefficients, as shown in Table 2.

B. SIMULATION AND TEST RESULTS ANALYSIS

During the PST shift process, the drive current of the solenoid valve is easy to measure, and its change can effectively reflect the change of the clutch torque. Therefore, we use the change of the drive current to analyze the clutch engagement law in the simulation and test, as shown in Fig. 9.

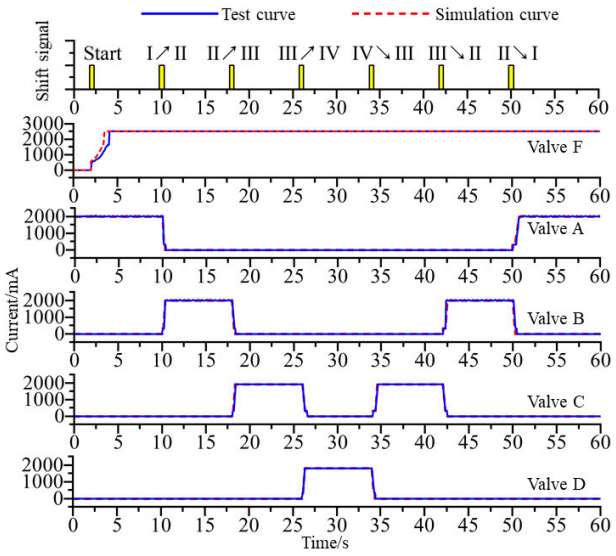

FIGURE 9. Comparison of simulation and test results of shift solenoid valve drive current.

In Fig. 9, the ordinate represents the drive current of the shuttle solenoid valve F and the shift solenoid valves A, B, C, and D. The simulation and test curve change trends are basically the same. Before the forward start command is issued, the drive current of the shift solenoid valve A has reached 2000mA, and the clutch has been engaged, which is consistent with the start strategy. The start strategy requires that when the system oil pressure reaches 22bar, the lowest gear shift clutch is engaged and waiting for the shuttle command. When the clutch is engaged as the tractor is stationary, it takes a short time and does not produce sliding friction, which can increase its life.

To specifically get the changes of shift solenoid valve drive current at the shift point, the drive current of the two clutches

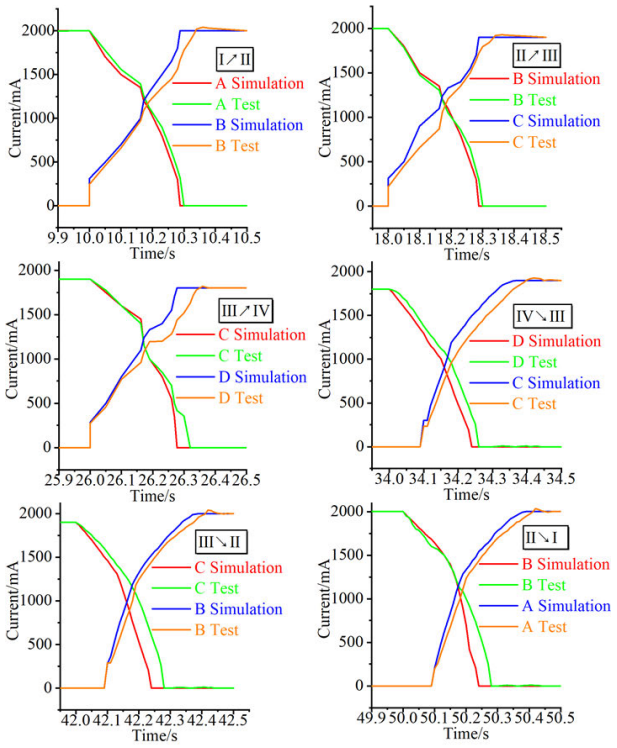

FIGURE 10. Shift solenoid valve drive current at shift point.

involved at the shift point in Fig. 9 is taken for analysis. Fig. 10 shows the simulation and test results.

The gear shift time is the sum of the time spent in the preparation phase, sliding friction phase and holding phase, which can be calculated using (26).

$$t_S = t_P + t_{SF} + t_H \tag{26}$$

In (26), t_S is the shift time, s, t_P is the time spent in preparation phase, s, t_{SF} is the time spent in sliding friction phase, s, and t_H is the time spent in holding phase, s.

Table 3 shows the shift time at the shift point in the upshift and downshift conditions.

TABLE 3. Comparison of shift time between simulation and test.

Condition	Simulation(s)	Test(s)	Error
I↗II	0.29	0.31	6.45%
II↗III	0.29	0.31	6.45%
III↗IV	0.30	0.32	6.25%
IV↘III	0.35	0.37	5.41%
III↘II	0.35	0.38	7.89%
II↘I	0.36	0.38	5.26%

According to Table 3, the upshift time is shorter than the downshift time. The reason is that when downshifting, the engagement of the clutch is delayed after receiving the shift command. The maximum error between shift time simulation and test data appears at the third gear downshift point, the error value is 7.89%, which is less than 10%, and the data has high accuracy. The minimum correlation coefficient between the simulation and the test data of the solenoid valve drive current at all shift points is 0.92, and the corresponding level is 5, indicating that the correlation degree is the biggest, the clutch engagement law simulation data is consistent with the test data, thus the PST system simulation model is accurate.

V. CONCLUSION

1) The PST architecture modeling and HLA-based PST simulation system structure were analyzed based on architecture modeling and HLA principles.

2) The simulation models of PST mechanical, hydraulic and control subsystems were established based on the analysis of PST system dynamics principles. Then the simulation component of each subsystem was built based on HLA, the mapping relationship between the simulation components was analyzed, the interfaces between the simulation components and the system were encapsulated, and the PST system simulation model was established.

3) The PST clutch engagement law under tractor shift conditions was simulated and tested, using the relative error and correlation coefficient between the simulation and the test data of the solenoid valve drive current to evaluate the PST system simulation model accuracy. The results showed that the simulated shift solenoid valve drive current is consistent with the test curve overall, the maximum error between the simulated shift time and the test result appears at the third gear downshift point, the error value is less than 10%, and the data has high accuracy. The minimum correlation coefficient between the solenoid valve drive currents at all the simulated shift points and the test results is 0.92, indicating that the simulated clutch engagement law is consistent with the test results, and the PST system simulation model is effective and accurate.

The modeling method of tractor PST in this paper can improve the model reusability, the system scalability and verification performance, and can effectively ensure the model accuracy.

REFERENCES

[1] Z. Q. Xi, Z. L. Zhou, and M. Z. Zhang, "Application analysis of automatic powershift transmission on tractor," *Mach. Des. Res.*, vol. 30, no. 2, pp. 140–143, 2014.

[2] T. Lin, X. Chai, and B. Li, "Top-level modeling theory of multi-discipline virtual prototype," *J. Syst. Eng. Electron.*, vol. 23, no. 3, pp. 425–437, Jun. 2012.

[3] X. F. Yan, G. L. Duan, and H. J. Xu, "Virtual prototyping technology oriented to complex mechatronic system," *CIMS*, vol. 20, no. 11, pp. 2652–2659, 2014.

[4] X. Ye, Q. Pan, and Z. H. Dong, "Comparison of multi-domain modeling and simulation technology," *Comput. Eng. Soft.*, vol. 35, no. 3, pp. 233–236, 2014.

[5] M. Tanelli, G. Panzani, S. M. Savaresi, and C. Pirola, "Transmission control for power-shift agricultural tractors: Design and end-of-line automatic tuning," *Mechatronics*, vol. 21, no. 1, pp. 285–297, Feb. 2011.

[6] S. Raikwar, V. K. Tewari, S. Mukhopadhyay, C. R. B. Verma, and M. S. Rao, "Simulation of components of a power shuttle transmission system for an agricultural tractor," *Comput. Electron. Agricult.*, vol. 114, pp. 114–124, Jun. 2015.

[7] B. Li, D. Sun, M. Hu, and J. Liu, "Automatic starting control of tractor with a novel power-shift transmission," *Mechanism Mach. Theory*, vol. 131, pp. 75–91, Jan. 2019.
[8] B. Li, D. Sun, M. Hu, X. Zhou, J. Liu, and D. Wang, "Coordinated control of gear shifting process with multiple clutches for power-shift transmission," *Mechanism Mach. Theory*, vol. 140, pp. 274–291, Oct. 2019.
[9] Z. Q. Xi, Z. L. Zhou, and M. Z. Zhang, "Shift characteristics and control strategy of powershift transmission on tractor," *Trans. Chin. Soc. Agric. Mach.*, vol. 47, no. 11, pp. 350–357, 2016.
[10] Z. Q. Xi, "Study on control system of tractor powershift transmission," Ph.D. dissertation, Sch. Mech. Precis. Instrum. Eng., Xi'an Univ. Technol., Xi'an, China, 2016.
[11] D. Q. Wang, "Study on the performance of agricultural tractor powershift transmission," Ph.D. dissertation, Coll. Eng., China Agr. Univ., Beijing, China, 2014.
[12] F. Zhang, "Distributed collaborative modeling and simulation technology of digital performance prototype for aerospace products," Ph.D. dissertation, Sch. Autom, NPU, Xi'an, China, 2015.
[13] J. Peng, J. Shi, L. Y. Zhang, F. H. Cai, and C. Xu, "Research and implementation of vehicle virtual test system based on product performance prototype," *Comput. Meas. Control*, vol. 25, no. 4, pp. 233–236, 2017.
[14] X. Y. Li, X. X. Huang, Y. Long, and Z. L. Zhang, "Development of surface-to-surface missile operation training simulation system based on HLA," *J. Syst. Simul.*, vol. 20, no. 21, pp. 5821–5824, 2008.
[15] Y. Liu, L. Zhang, and Y. Laili, "Study on model reuse for complex system simulation," *Scientia Sinica Informationis*, vol. 48, no. 7, pp. 743–766, Jul. 2018.
[16] W. Y. Cai, X. Li, S. H. Wan, and W. L. Wang, "Framework of modeling and simulation for aerial defense radar early warning surveillance system and its implement," *J. Syst. Simul.*, vol. 24, no. 3, pp. 688–691, 2012.
[17] A. Falcone, A. Garro, A. Anagnostou, and S. J. Taylor, "An introduction to developing federations with the High Level Architecture (HLA)," in *Proc. WSC*, Las Vegas, NV, USA, Dec. 2017, pp. 617–631.
[18] M. Gutlein, R. German, and A. Djanatliev, "Towards a hybrid co-simulation framework: HLA-based coupling of MATSim and SUMO," in *Proc. IEEE/ACM 22nd Int. Symp. Distrib. Simul. Real Time Appl. (DS-RT)*, Oct. 2018, pp. 1–9.
[19] T. Nagele and J. Hooman, "Co-simulation of cyber-physical systems using HLA," in *Proc. IEEE 7th Annu. Comput. Commun. Workshop Conf. (CCWC)*, Jan. 2017, pp. 1–6.
[20] H. K. Jun and Y. I. Eom, "Interoperable middleware gateway based on HLA and DDS for L-V-C simulation training systems," *IEMEK J. Embedded Syst. Appl.*, vol. 10, no. 6, pp. 345–352, Dec. 2015.
[21] B. Xiao and T. Y. Xiao, "Extending HLA/RTI for dynamical reusability of federates," *J. Tsinghua Univ., Sci. Technol.*, vol. 54, no. 3, pp. 326–333, 2014.
[22] X. Lin and R. Z. Jia, "Modeling of FOM/SOM development process," *J. Syst. Simul.*, vol. 18, no. S2, pp. 332–336, 2006.
[23] Y. Wang, H. W. Li, and L. Y. Sun, "Research and improvement of time management algorithm in high level architecture," *Comput. Eng.*, vol. 39, no. 1, pp. 279–282, 2013.
[24] J.-B. Chaudron, D. Saussié, P. Siron, and M. Adelantado, "Real-time distributed simulations in an HLA framework: Application to aircraft simulation," *Simulation*, vol. 90, no. 6, pp. 627–643, Jun. 2014.
[25] Z. Q. Xi, Z. L. Zhou, and M. Z. Zhang, "Research of economical shift rule of automatic power shift transmission of tractor," *J. Mech. Transm.*, vol. 40, no. 11, pp. 144–150, 2016.

WU YIWEI received the B.S. and M.S. degrees in vehicle engineering from the Henan University of Science and Technology, Luoyang, China, in 2013 and 2016, respectively, where he is currently pursuing the Ph.D. degree in vehicle engineering. His research interests include digital design of agricultural vehicles, man-machine systems design, collaborative modeling, and simulation of multidisciplinary virtual prototyping. He is a member of CSAE.

YAN XIANGHAI received the B.S., M.S., and Ph.D. degrees in vehicle engineering from the Henan University of Science and Technology, Luoyang, China, in 2009, 2013, and 2020, respectively. He is currently a Lecturer with the Henan University of Science and Technology. He has rich practical experience in the field of vehicle test. His main research direction is vehicle test method and technology. His research interests include the power matching of the transmission system of agricultural and road transport vehicles, and the design and test of steering control. He is a member of CMES.

ZHOU ZHILI received the Ph.D. degree in tractor specialty from the Jilin University of Technology (now Jilin University), Changchun, China, in 1993.

He is currently a Professor and a Doctoral Supervisor. He is also the Director of the Henan Key Laboratory of Vehicle Energy Saving and New Energy, the Director of the Key Open Laboratory of Vehicle Engineering Discipline of Henan Education Department, the Director of CMES, the Executive Director of CSAM and CSAE, and the Honorary Chairman of the Henan Mechanical Engineering Society. Since 2002, he has been the Vice President of the Henan University of Science and Technology, Luoyang, China. He is the author of eight books and more than 100 articles. He presided over or participated in more than 40 national and provincial projects and won six provincial and ministerial science and technology progress awards. His research interests include vehicle transmission theory and control, vehicle system dynamics, vehicle virtual design and test, and vehicle performance analysis and simulation technology. He serves on the Editorial Board of Transactions of the CSAE and CSAM.